SLAC-26
UC-28, Particle Accelerators
and High-Voltage Machines
UC-34, Physics
TID-4500

DYNAMIC FIELD MEASUREMENTS WITH AN EMR MAGNETOMETER IN THE PULSED BEAM SWITCHING MAGNET

February 1964

by

J. J. Muray and R. A. Scholl

Technical Report
Prepared Under
Contract AT(04-3)-400
for the USAEC
San Francisco Operations Office

Printed in USA. Price $ .50. Available from the Office of Technical Services, Department of Commerce, Washington 25, D.C.

TABLE OF CONTENTS

LIST OF FIGURES

I. INTRODUCTION

The electron beam from the Stanford two-mile linear accelerator is analyzed by a high quality magnetic deflection system in the beam switchyard. The basic elements of the magnetic transport systems with the calculated beam profiles are shown in Fig. 1. The first magnet element in this system is a pulsed switching magnet capable of switching beams of different energies and intensities to either transport system on a pulse-to-pulse basis. This magnet actually consists of five 1-meter sections and is powered by pulsed high voltage supplies (modulators). Each magnet section is excited with two modulators because it should be able to pulse in either polarity in order to switch the beam left or right; the pulse height should be continuously variable to accommodate any beam energy. The magnetic field in these magnets rises sinusoidally 360 times a second and has a peak value at 2070 gauss. The details of the pulsed magnet system are described elsewhere.[1]

II. OPTICS OF THE PULSED MAGNET

The optical transfer matrix for the deflection system from the exit of the pulsed magnet to the energy defining slit has the form

$$\begin{pmatrix} X \\ \theta \end{pmatrix}_{\substack{\text{Quad}\\ \text{Input}}} = \begin{pmatrix} M_{11} & 0 \\ M_{21} & M_{22} \end{pmatrix} \begin{pmatrix} X_o \\ \theta_o \end{pmatrix}_{\substack{\text{Machine + Pulsed magnet}\\ \text{Output}}}$$

which shows that a change in the input divergence angle θ_o into the deflection system does not change the focusing condition or the energy resolution in first-order optics. This means that the deflection system is decoupled from the pulsed magnet and the accelerator, and a change in the divergence angle due to a small amplitude variation in the magnetic field of the pulsed magnet will not influence the focusing conditions. The limit for the maximum variation in θ_o is set by the aperture size of the input quadrupole of the deflection system. Because the half aperture size is 4 cm and the half beam width is 2 cm, the offset distance for the beam

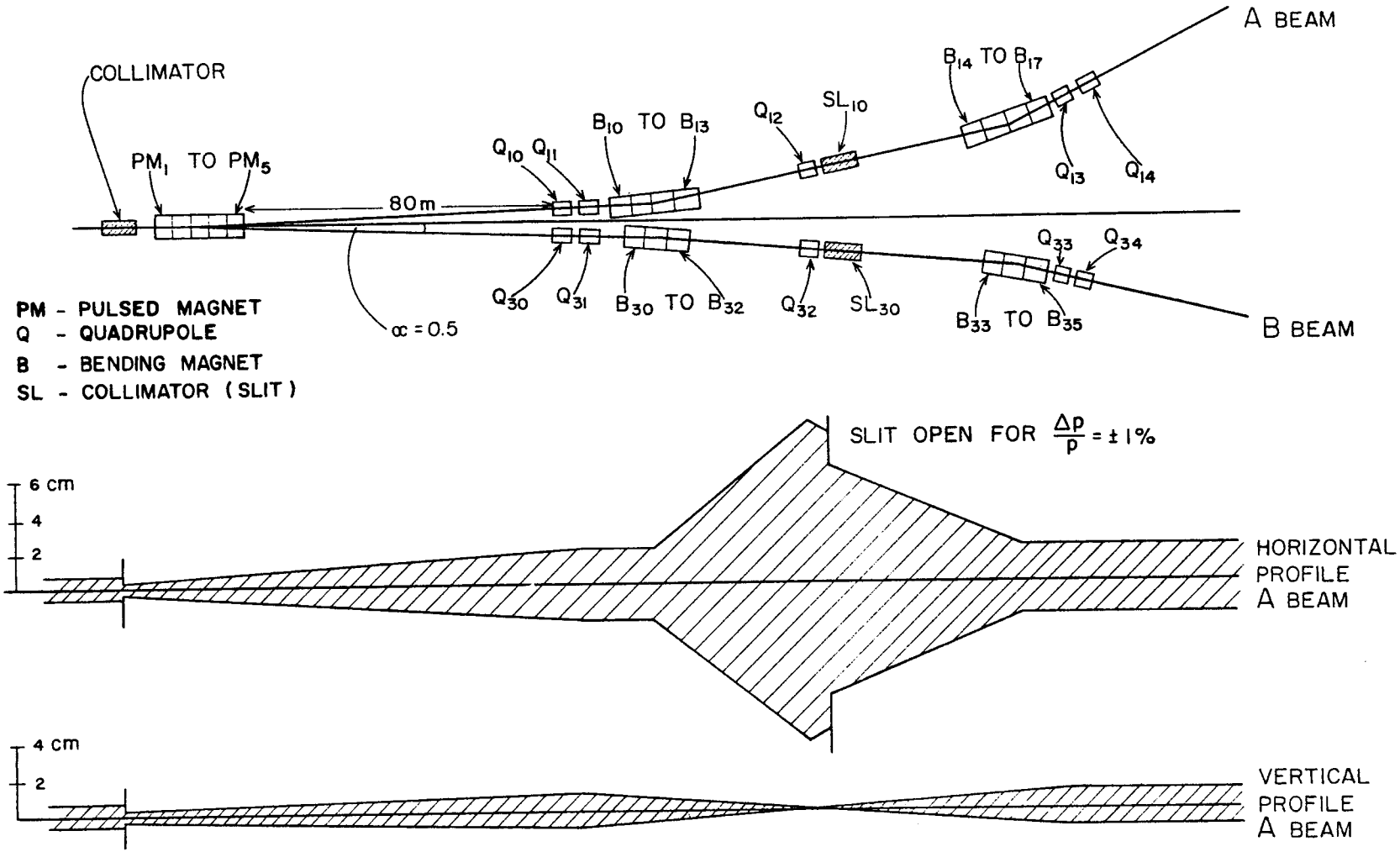

FIG. I SCHEMATIC LAYOUT OF THE BEAM SWITCHYARD AND PROFILES OF THE A BEAM

should be less than ±2 cm. However, the change in the offset distance, b, is proportional to the change in magnetic field. The maximum for this system can be calculated from the formula

$$\delta b(\text{cm}) = 8000 \times \frac{0.5}{57} \times \frac{\Delta B}{B}$$

If $\delta b = \pm 2$ cm, then $\frac{\Delta B}{B} = 2.65 \times 10^{-2}$; using for the peak field $B = 2070$ gauss, the field in the pulsed magnet can change ±55 gauss.

There is one other way to estimate the field stability in the pulsed magnet. In this case one actually tries to separate from the total beam divergence θ_o the divergence due to the accelerator itself (θ_1) and the part which is due to the pulsed magnet (θ_M). Computer calculations have verified[2] that to achieve a 0.3-cm image spot at the collimator, the total divergence of the beam should be less than 3×10^{-4} radians. (For a point spot the maximum possible divergence is 4.2×10^{-4} radians.) In order to estimate θ_M, let us suppose that the beam has a gaussian intensity distribution at the end of the accelerator. Let $\sigma\theta_1$ be the standard deviation of the beam divergence before the pulsed magnet, $\sigma\theta_o$ be the standard deviation of the total beam divergence after the pulse magnet, and $\sigma\theta_M$ be standard deviation of the beam divergence introduced by the pulsed deflecting magnet.

Then, in order to pass three deviations in beam divergence in the deflecting system, the total divergence is $\sigma\theta_o \leq 1 \times 10^{-4}$, i.e.,

$$(\sigma\theta_o)^2 = (\sigma\theta_M)^2 + (\sigma\theta_1)^2 \leq 1 \times 10^{-4}$$

or

$$\sigma\theta_M \leq \left[(\sigma\theta_o)^2 - (\sigma\theta_1)^2\right]^{\frac{1}{2}}$$

Because $\frac{\theta_M}{\alpha} = \frac{\Delta B}{B}$ where $\alpha = 0.5^o$, then

$$\sigma\left(\frac{\Delta B}{B}\right) = \sigma\left(\frac{\theta_M}{\alpha}\right) = \frac{\sigma\theta_M}{\alpha}$$

This gives an rms error tolerance for $\frac{\Delta B}{B}$ of

$$\sigma\left(\frac{\Delta B}{B}\right) \leq \frac{\left[(\sigma\theta_o)^2 - (\sigma\theta_1)^2\right]^{\frac{1}{2}}}{\alpha}$$

If, for example, the beam divergence from the accelerator is $\sigma\theta_1 = 1 \times 10^{-5}$, then

$$\sigma\left(\frac{\Delta B}{B}\right) \approx 1.2 \times 10^{-2} \quad \text{or} \quad 1\% \text{ rms}$$

However, if $\sigma\theta_1 = 1 \times 10^{-5}$, the $\sigma\theta_M$ should be zero.

Using a uniform intensity distribution for the electron beam from the machine, one obtains

$$\left|\frac{\Delta B_{max}}{B}\right| \leq \frac{1}{\alpha}\left[|\theta_o| - |\theta_1|\right]$$

Then, for example, using $|\theta_o| = 3 \times 10^{-4}$ and $\theta_1 = 3 \times 10^{-5}$, the result is

$$\left|\frac{\Delta B_{max}}{B}\right| \leq 3.2 \times 10^{-2}$$

From this one can conclude that the peak field regulation does not need to be better than ±1%. However, to measure the field variation on a pulse-to-pulse basis one would like to use a field measuring instrument with an accuracy of better than 0.1%. With such an instrument one would also be able to measure the variation of the remnant field, which is less than ±2 gauss. Therefore, an instrument capable of measuring dynamic magnetic fields with reasonably high accuracy was needed both to calibrate other measurement equipment and for use as a test instrument for a pulsed magnet modulator. Absolute accuracy of 0.05% (worst case) was desired. The field to be measured consisted of a half cycle of a 1000 cps sine wave with a peak field of about 2 kG. Eddy current losses in

metal precluded the use of probes that presented large metal surfaces to the magnetic field because distortions would be introduced into the field, with resultant heating of the probe.

Electron magnetic resonance of the organic free radical 1,1 Diphenyl 2, Picryl Hydrazil (DPPH) was chosen as a measurement method. DPPH has a linewidth of 1.35 gauss, a relaxation time of about 0.2 μsec, and a g-value of 2.0036 ±0.0002.[3]

With the g-value of DPPH, the resonance frequency is given by $F = (2.804 \pm 0.001)B$,[4] where F is the frequency in Mc and B_o is the field in gauss.

Therefore, fields of 1400 to 2100 gauss will resonate with microwave signals from 3.95 to 5.85 kMc, the "G" band region.

A helix slow wave structure was chosen as the microwave flux concentrator because it did not support large eddy currents and its frequency independence allows the use of large sample volumes without the normal pulling present in high-Q cavities, which tends to broaden the resonance line.

III. FIELD MEASURING SYSTEM

A simple microwave bridge was used in the detection system (see Fig. 2). The klystron output was fed to the hybrid tee, which divides the power between the helix and the attenuator-phase shifter-short combination. The latter reflects a signal which is 180° out of phase with the reflection from the probe, and has suitable amplitude to bias the crystal detector to a low noise region. When resonance occurs, the amplitude and phase of the reflected signal from the helix are modified, and the bridge is unbalanced. The resulting rf pulse sent to the crystal is amplified and presented to the vertical deflection plates of the oscilloscope.

IV. ELECTRON MAGNETIC RESONANCE (EMR) MAGNETOMETER

The power source consisted of a 2K43 klystron, air cooled. Conventional waveguide components were used throughout, except for the probe.

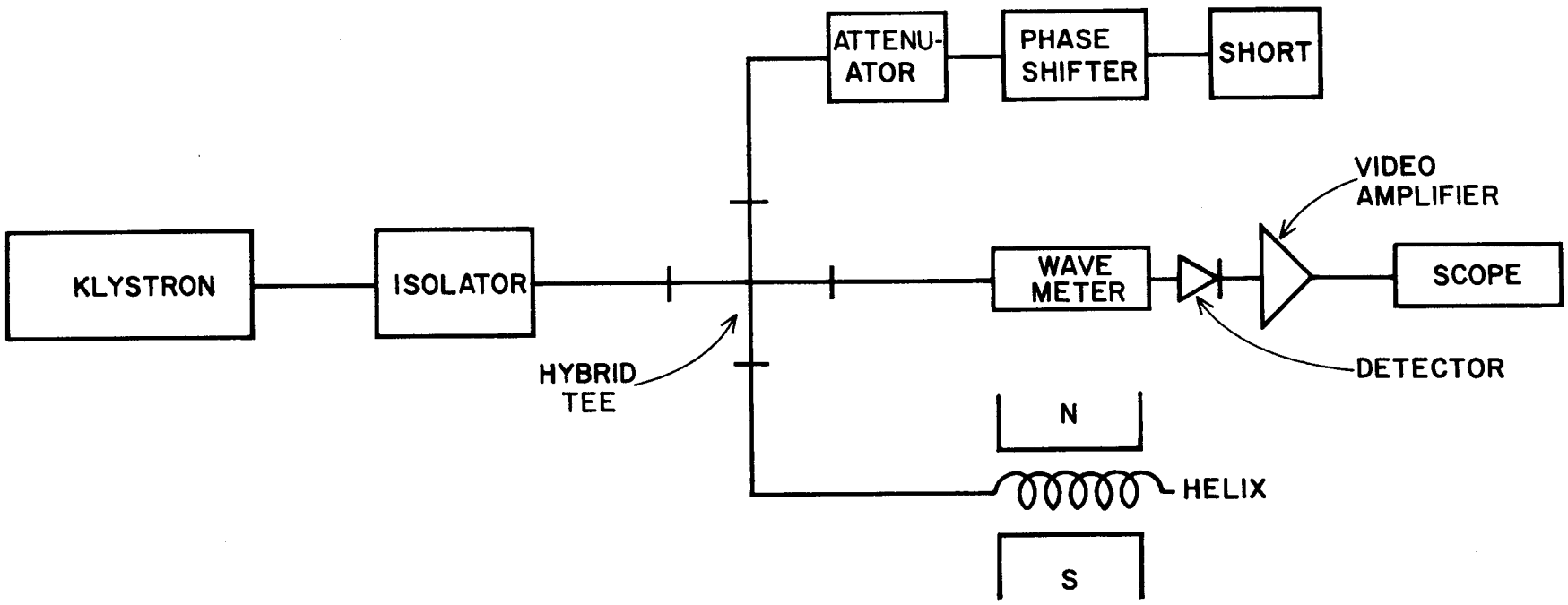

FIG. 2--Diagram of the magnetic field measuring system.

As mentioned above, the probe could not present a large metal surface to the field, and for this reason high-Q resonant cavities were not used. Webb[5] suggested the use of traveling wave helices in place of metallic or dielectric cavities for this purpose.

The helix was designed on the basis of a simplified theory. For a more general analysis the reader is referred to Pierce.[6] The microwave magnetic field in the helix is

$$H = \mu_o nI$$

where n is the number of turns/meter and I is the current in the helix. In terms of the magnetic field inside the helix and the helix radius a, the input power to the helix can be written as

$$P_I = U\pi a^2 V_p$$

where $U = \frac{H^2}{2\mu_o}$, the energy density in the helix. Therefore,

$$P_I = \frac{1}{2\mu_o} H^2 a^2 V_p$$

The velocity of propagation is given by

$$V_p = c/2\pi na ,$$

where c = velocity of light in vacuum. Then, using $H = \mu_o nI$,

$$P_I = \frac{1}{4} \mu_o nacI^2$$

The wave impedance is given by

$$P_h = Z_h I^2$$

where P_h is the power <u>inside</u> the helix. Because only half of the wave

power is inside the helix, $P_I = 2P_h$, and

$$Z_h = \frac{P_{I/2}}{I^2} = \frac{1}{8}\mu_o nac = 15\ \pi na$$

For a 52-ohm helix, it is required that

$$na = \frac{52}{15\pi} = 1.10$$

Defining $\beta_o = 2\pi/\lambda_o$ and $\beta = 2\pi/\lambda$, where λ_o is the free space wavelength and λ the helix wavelength, we must have

$$1 \leq \beta a \leq 1.5$$

in order that the lowest mode be propagated (i.e., a mode in which the magnetic field is not a function of θ). Assuming as before that the wave flows around the helix with velocity c gives

$$\beta = 2\pi na\beta_o$$

For a 52-ohm helix,

$$\beta = 7.26$$

Taking $\beta a = 1$ yields

$$a = 0.138 \text{ cm}$$

$$n = 8 \text{ cm}^{-1}$$

The probe assembly consisted of a small 50-ohm helix coupled to a narrower 90-ohm helix containing the sample. The sample helix was long enough to extend into the pulsed magnet. In accordance with the above results, the coupling helix had an internal diameter of 0.276 cm and 7.97 turns per centimeter. The sample helix was 20.32 cm long, 0.15 cm in diameter, and had 24.4 turns/cm. The coupling helix was terminated with a 1/10-watt, 50-ohm resistor imbedded in the matching structure. See Fig. 3 for

structural details, and Fig. 4 for a photograph of the completed probe in its supporting structure.

An IN23B crystal was used as the detector in all of the studies. The demodulated resonance signal was amplified 20 db by a Hewlett-Packard Model 466A video amplifier and presented to a Tektronix 545A oscilloscope.

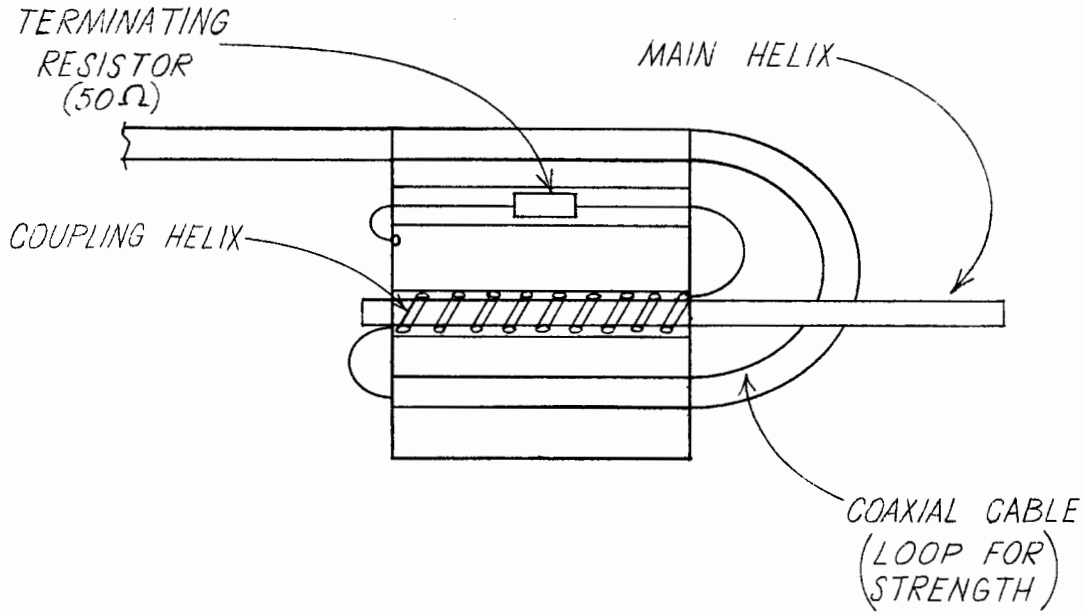

FIG. 3--Cutaway view of helix coupler.

V. MEASUREMENTS

The SLAC pulsed magnet power supply operates by switching a capacitor, charged to 5 kV, across the magnet coils. The resultant resonant circuit rings through one half cycle. The capacitor, now charged in the reverse polarity, is then switched across a second coil that is designed to be electrically similar to the magnet. The circuit again rings through one half cycle, returning the capacitor to the original polarity but somewhat lower voltage due to ohmic and core losses. The capacitor is then resonant charged to its original voltage by a third switch. Precise control of the capacitor voltage is accomplished by "Q-spoiling," or shorting of the second (dummy) coil, when the capacitor voltage reaches a preset level. All switching is accomplished with high power ignitrons. See Fig. 5 for basic circuit and waveforms.

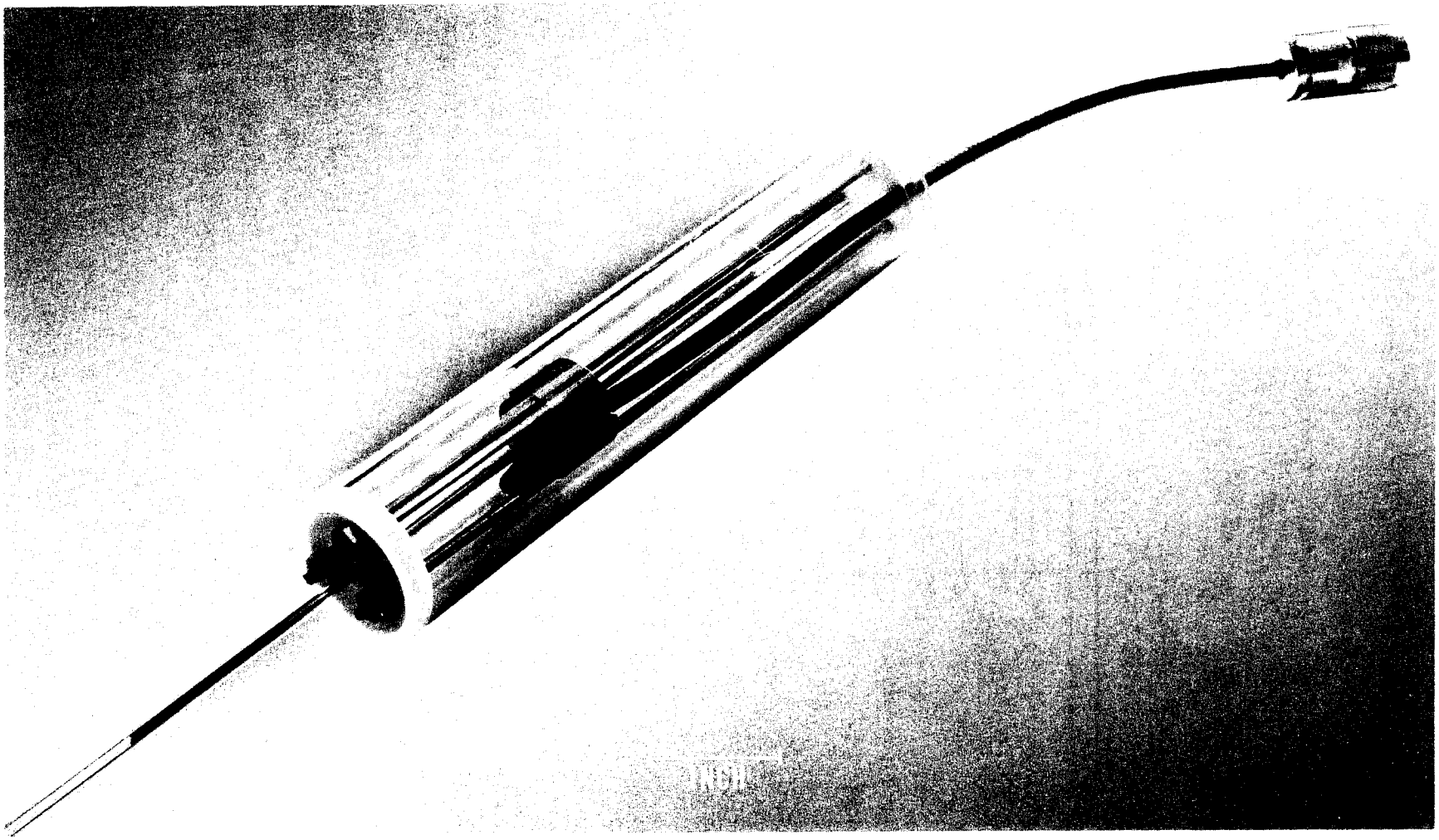

FIG. 4--Probe assembly.

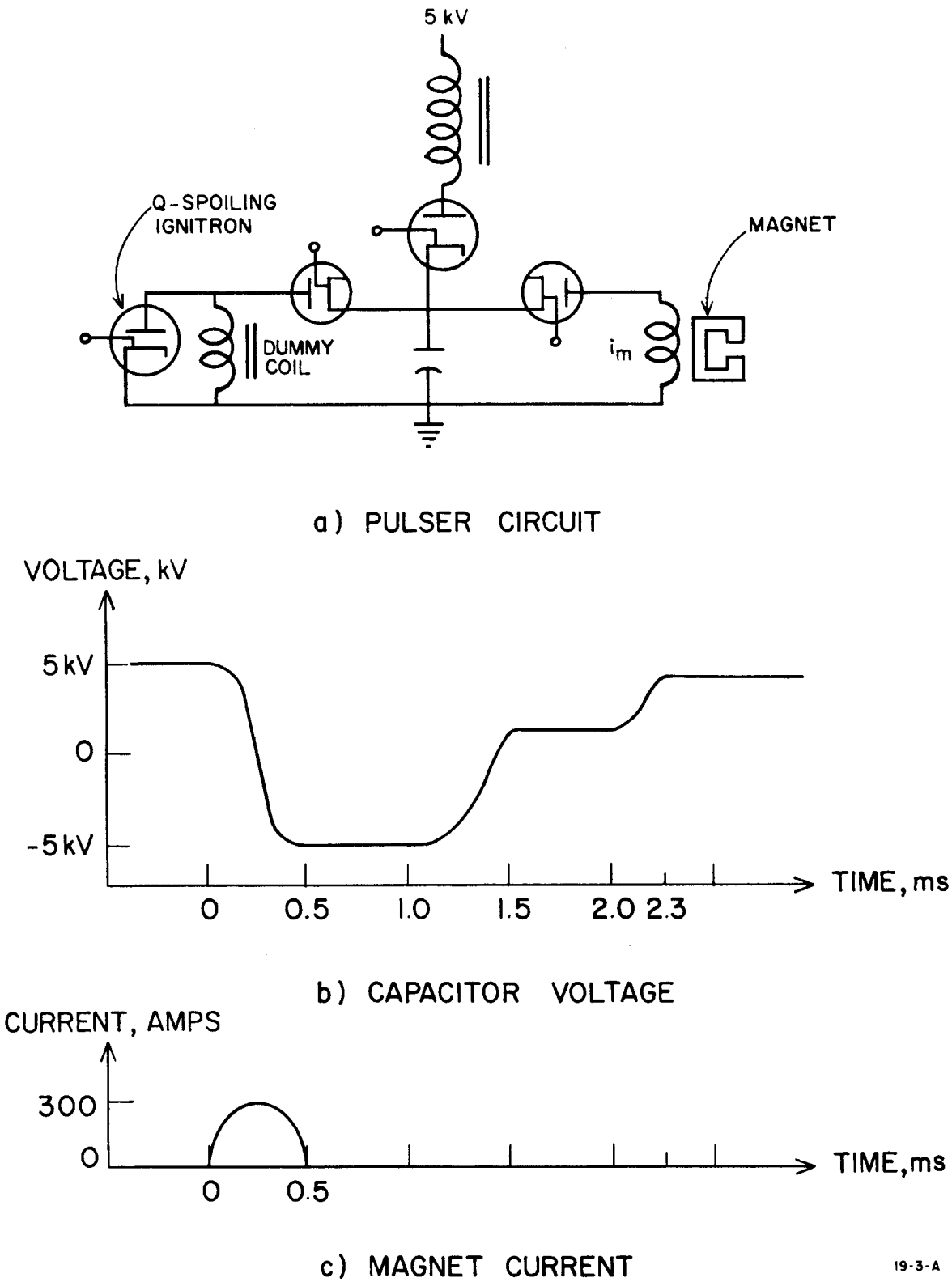

FIG. 5--Basic pulser circuit and waveforms.

Because the capacitor voltage, and thus the magnet current, is a critical function of the firing time of the "Q-spoiling" ignitron, time jitter in its firing caused amplitude jitter in the magnetic field. The primary measurement made on the SLAC pulsed magnet was the amplitude jitter in the magnetic field.

Since the field waveform was a sine function, two signals were obtained from the EMR system during each field pulse, one during field rise and one upon field fall. These signals are equally spaced about the peak field. The amplitude jitter was measured by measurement of the relative jitter between these two pulses. The relationship between time and amplitude jitter is developed as follows.

Let $H = H_o \sin \omega\tau$. Because the EMR pulses are equally spaced about the peak field, the times τ_1 and τ_2 of these pulses are related by (See Fig. 6) $\tau_1 + \tau_2 = T/2$ where T is the sine period.

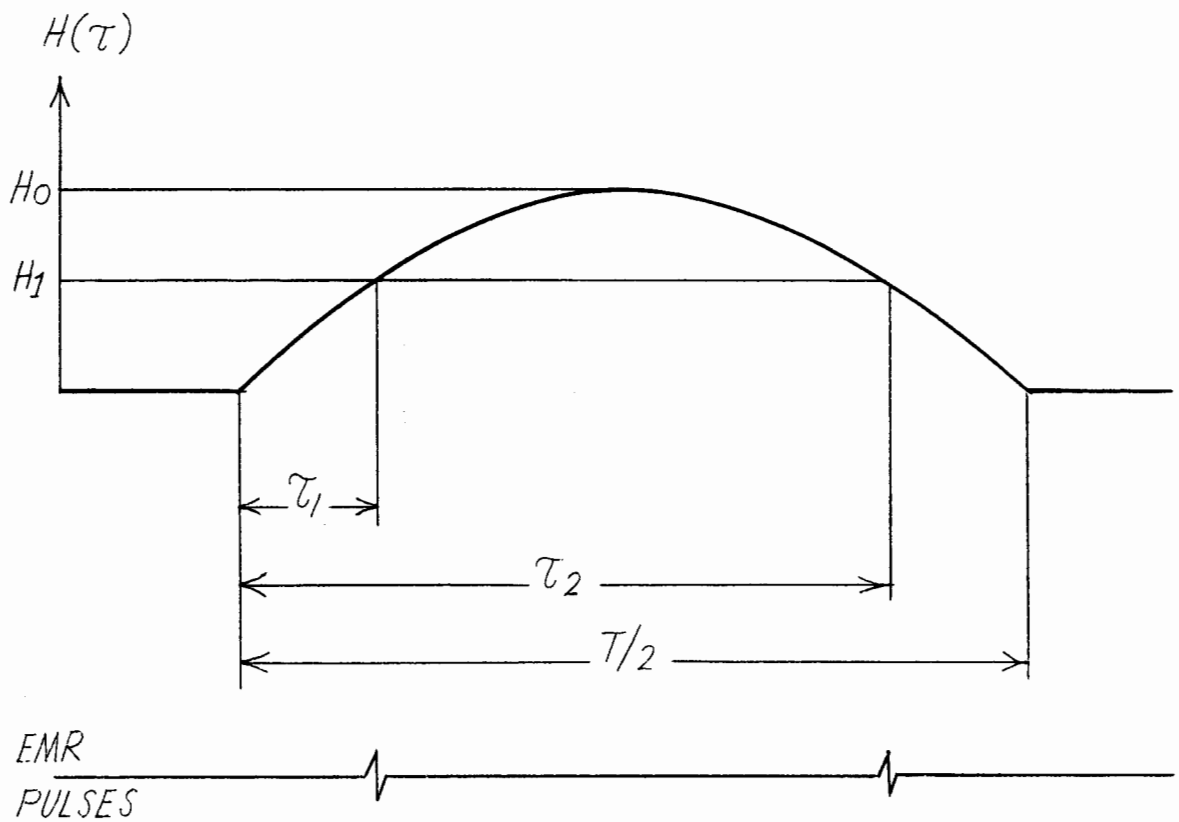

FIG. 6--Pulse timing diagram.

Let $\Delta\tau = \tau_2 - \tau_1$; then $\tau_1 = \frac{1}{2}(T/2 - \Delta\tau)$. If H_1 is the field at time τ_1 , then

$$H_1 = H_o \sin \frac{\omega}{2} [T/2 - \Delta\tau]$$

and

$$H_o = \frac{H_1}{\sin \frac{\omega}{2} (T/2 - \Delta\tau)}$$

Suppose $\Delta\tau$ changes by δ . Then, assuming the same H_1 , the new value for the peak field is

$$H_o' = \frac{H_1}{\sin \frac{\omega}{2} (T/2 - \Delta\tau - \delta)}$$

The change in the field is

$$\Delta H_o = \frac{H_1}{\sin \frac{\omega}{2} (T/2 - \Delta\tau - \delta)} - \frac{H_1}{\sin \frac{\omega}{2} (T/2 - \Delta\tau)}$$

and the fractional change in the field is

$$\frac{\Delta H_o}{H_o} = \frac{\sin \frac{\omega}{2} (T/2 - \Delta\tau)}{\sin \frac{\omega}{2} (T/2 - \Delta\tau - \delta)} - 1$$

Now $\frac{\omega}{2} \cdot \frac{T}{2} = \pi/2$. Thus $\frac{\Delta H_o}{H_o}$ becomes

$$\frac{\Delta H_o}{H_o} = \frac{\cos \omega\Delta\tau/2}{\cos \frac{\omega}{2} (\Delta t + \delta)} - 1$$

Assuming $\frac{\omega}{2}\delta \ll 1$, expansion of the denominator yields

$$\frac{\Delta H_o}{H_o} \approx \frac{\omega\delta}{2} \tan \frac{\omega\Delta\tau}{2} \qquad \left(\frac{\omega}{2}\delta \ll 1\right)$$

During the measurement sequence, $\frac{\omega\Delta\tau}{2}$ was made to be $\pi/6$, so that for the measurements $\tan \frac{\omega\Delta\tau}{2} = \frac{1}{\sqrt{3}}$, and

$$\left.\frac{\Delta H_o}{H_o}\right|_{\omega\Delta\tau=\pi/3} = \frac{\omega\delta}{2\sqrt{3}}$$

The value $\omega = 2000\pi$ yields

$$\left.\frac{\Delta H}{H_o}\right|_{\omega\Delta\tau=\pi/3} = 1810\delta$$

and 1 μsec of relative jitter corresponds to an amplitude jitter of 0.18%.

During the measurements, the probe assembly was mounted on a clamp and ring stand and positioned in a model of a pulsed magnet. The magnet was pulsed with the power supply and the EMR signals were observed on a Tektronix type 545A oscilloscope. Figure 7 shows the test setup. The EMR signals observed are shown in Figs. 8 through 11. In Fig. 8, the two EMR signals are shown on the lower trace. The upper trace is approximately proportional to the magnetic field; its lack of symmetry is due to overloading in the monitor circuitry. Horizontal sweep speed is 50 μsec/cm. In Fig. 9 the two EMR signals are shown more clearly on an expanded time base (20 μsec/cm); note that the two signals are mirror images of each other. The EMR frequency in all photographs was 4786.8 Mc, corresponding to a field of 1706.8 gauss at resonance.

Amplitude jitter in the field was measured by triggering the 545A delaying sweep from the first EMR signal and observing the second signal with the delayed sweep. As mentioned above, for all such measurements

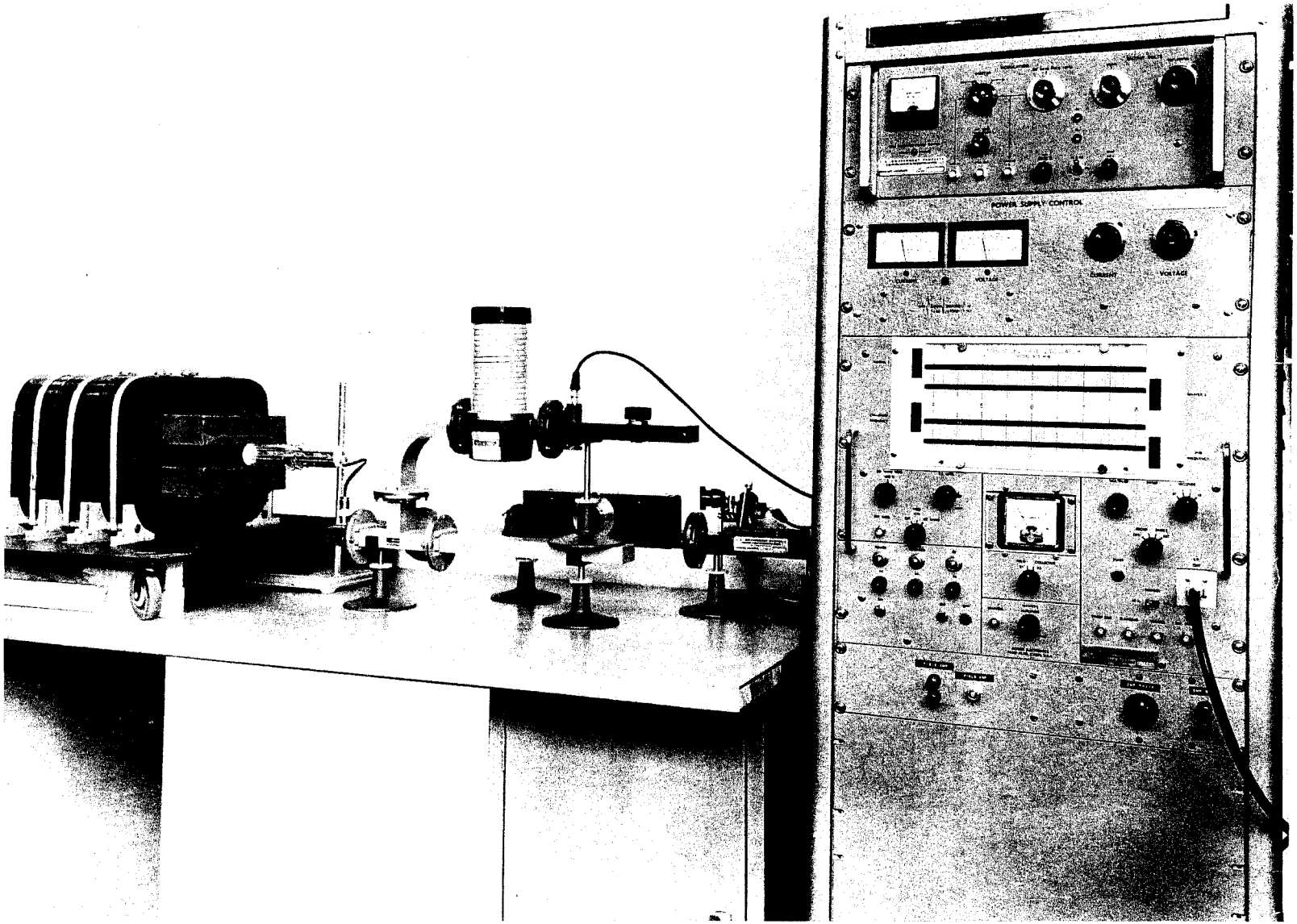

FIG. 7--Measurement test setup.

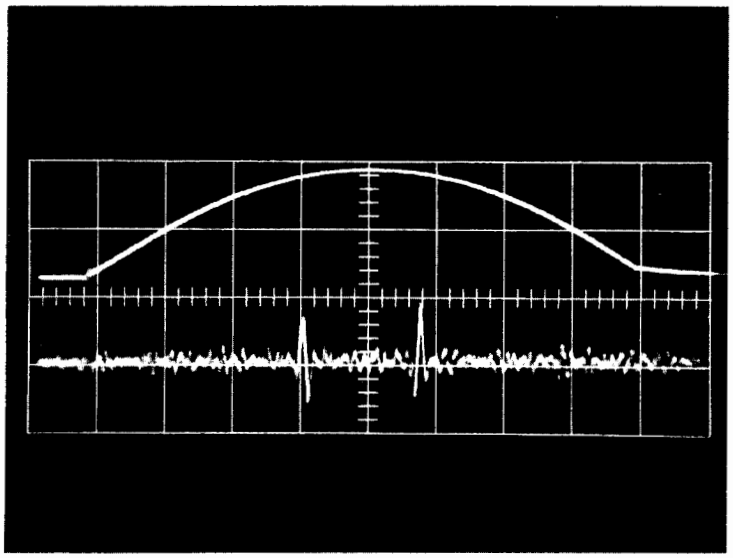

FIG. 8--Observed EMR signals at 50 μsec/cm sweep speed.

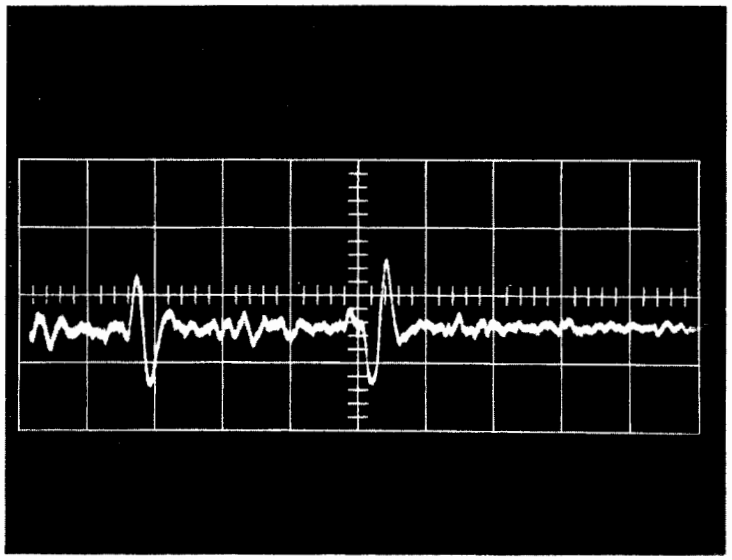

FIG. 9--Observed EMR signals at 20 μsec/cm sweep speed.

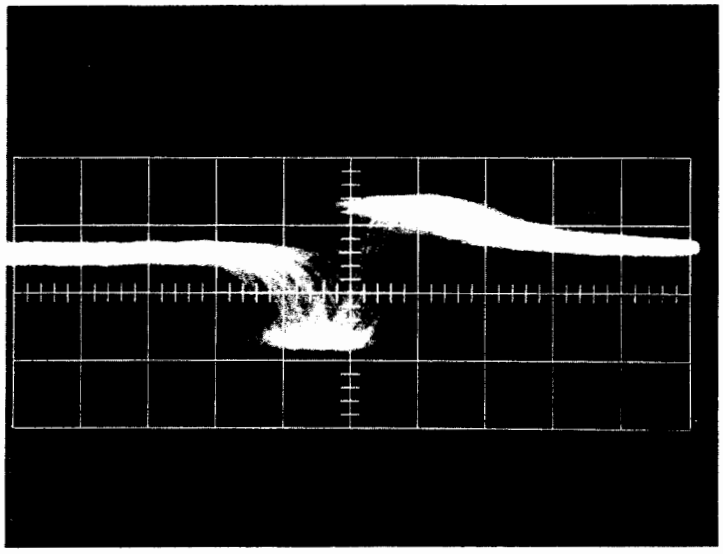

FIG. 10--Second EMR pulse, showing relative jitter with "Q-spoiling" circuit disconnected (2 μsec/cm).

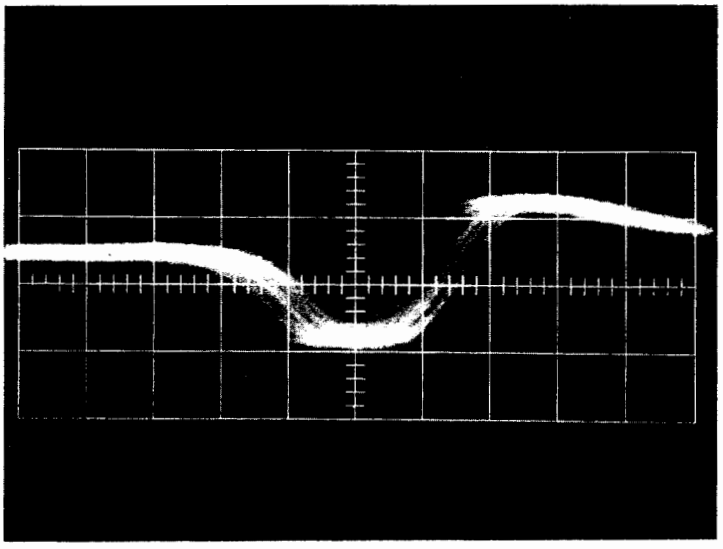

FIG. 11--Expanded second EMR pulse, showing effect of "Q-spoiling" on relative jitter (1 μsec/cm).

the signals were made to be 167 μsec apart ($\frac{\omega\Delta T}{2} = \pi/6$) in order to provide a common reference for the jitter measurements. Figure 10 shows the second EMR pulse on a time base of 2 μsec/cm. It should be noted that the more rapid rate of rise of the field at this point on the field waveform compresses the EMR signal in time as compared with the two earlier oscillographs. The total jitter is seen to be 4 μsec, corresponding to an amplitude jitter of about 0.7%, or 14 gauss for this peak field. This oscillograph was taken with the "Q-spoiling" circuits disconnected.

The effect of the "Q-spoiling" circuits can be seen by examination of Fig. 11. Here the second EMR pulse is shown on a time base of 1 μsec/cm. The peak-to-peak time jitter has been reduced to 1 μsec, corresponding to an amplitude jitter of 0.18%, or about 3.5 gauss.

VI. CONCLUSION

The EMR dynamic field magnetometer has been demonstrated to be an effective tool in the measurement of amplitude jitter in pulsed magnetic field waveforms. This instrument is a primary standard, and as such requires no calibration. Conventional means of measuring field jitter, such as a gated integrator and level detector combination, require constant calibration, and hysteresis and time jitter in the level detector itself limit the accuracy.

LIST OF REFERENCES

1. J. L. Cole, B. Hedin, and J. J. Muray, Internal Memorandum, Stanford Linear Accelerator Center, Stanford University, Stanford, California (January 1963).
2. C. H. Moore, S. K. Howry, and H. S. Butler, Internal Report, Stanford Linear Accelerator Center, Stanford University, Stanford, California (May 1963).
3. A. N. Holden *et al.*, Phys. Rev. *77*, (1950).
4. O. E. Spokas and M. Danos, Rev. Sci. Inst. *33*, 613 (June 1962).
5. R. H. Webb, Rev. Sci. Inst. *33*, 732 (July 1962).
6. J. R. Pierce, *Traveling Wave Tubes* (D. Van Nostrand Company, Inc., Princeton, N. J., 1950).